JOURNAL OF PROPULSION AND POWER
Vol. 24, No. 3, May–June 2008

Testing and Characterization of a Hydrogen Peroxide Monopropellant Thruster

A. Pasini,* L. Torre,† L. Romeo,‡ A. Cervone,§ and L. d'Agostino¶
ALTA S.p.A., 56121 Pisa, Italy

DOI: 10.2514/1.33121

In the present paper, the use of advanced catalytic beds on ceramic supports as a cost-effective alternative to metal screen reactors for the decomposition of high-concentration hydrogen peroxide in small monopropellant rockets is investigated. For this purpose, a reconfigurable test bench for the characterization of the operation and the propulsive performance of small rocket thrusters has been designed and realized. The present paper illustrates the experimental campaign carried out on a 5 N thruster prototype operating with two platinum catalysts on γ-alumina supporting spheres. The results indicated that Pt/Al_2O_3 is an effective catalyst combination for the decomposition of 87.5% propellant-grade hydrogen peroxide, with good stability and performance comparable to silver screen beds of equal geometric envelope and operational conditions. Incomplete hydrogen peroxide decomposition and the onset of flow oscillations in the reactor were observed at the tested levels of bed loading, residence time, and flow pressure. Thermal stresses due to the large temperature gradients occurring during the decomposition of high-grade hydrogen peroxide (87.5% by weight) caused the ceramic pellets to break and the progressive occlusion of the bed. Based on the analysis of the test results, several ways to overcome these problems in future investigations have been tentatively identified, together with the necessary modifications to the present experimental setup.

Nomenclature

A_t	=	throat area
C_F	=	thrust coefficient
c^*	=	characteristic velocity
F	=	thrust
g_o	=	sea level gravity acceleration
I_{sp}	=	specific impulse
$\dot{m}$	=	propellant mass flow rate
p_a	=	ambient pressure
p_c	=	combustion chamber pressure
R	=	gas constant of the exhaust gases
T_{ad}	=	adiabatic decomposition temperature
T_{amb}	=	ambient temperature
T_c	=	combustion chamber temperature
T_{exp}	=	decomposition temperature (experimentally measured)
γ	=	specific heat ratio of the exhaust gases
η_{c^*}	=	characteristic velocity efficiency
$\eta_{\Delta T}$	=	temperature efficiency

I. Introduction

IN THE last decade there has been a renewed interest in hydrogen peroxide (HP) engines, generated mainly by the need for less toxic and dangerous propellants. As a green propellant, hydrogen peroxide allows for a drastic simplification of the health and safety protection procedures needed in its production, storage, and handling. As a result, attractive savings can be obtained in low- or medium-thrust rocket engines for small missions, for which the overall cost of propulsion systems with traditional propellants does not scale down proportionally to the rocket size.

The nominal propulsive performance of hydrogen peroxide as a monopropellant is about 20% lower than hydrazine, but the volume specific impulse achievable with 90% H_2O_2 is higher than for most other propellants due to its high density. This is particularly useful for systems with significant aerodynamic drag losses or stringent volume constraints, as is often the case for small satellites. Finally, when used in bipropellant and hybrid rocket engines, hydrogen peroxide yields specific impulses comparable to other liquid oxidizers such as dinitrogen tetroxide, nitric acid, and even liquid oxygen (Wernimont and Muellens [1], Wernimont and Garboden [2]). Furthermore, with respect to other high-energy green propellants, such as ammonium dinitramide, hydroxylamine nitrate, and hydrazinium nitroformate (Wucherer et al. [3], Schoyer et al. [4]), hydrogen peroxide has the significant advantage that its decomposition temperature does not require the use of extremely expensive materials and manufacturing processes for the thrust chamber.

The earliest research on hydrogen peroxide-based rockets was conducted by Walter [5] in Germany during the 1930s. Interest in hydrogen peroxide in the postwar years up to about 1955 was confined largely to the United Kingdom, although both the United States and the former Soviet Union developed the Walter concept for different applications. A significant amount of work on hydrogen peroxide decomposition and its application to monopropellant rockets was carried out in the 1960s at NASA laboratories [6,7], but this effort was subsequently abandoned with the advent of effective hydrazine catalysts and engines. Nevertheless, the Russian Soyuz launch vehicle, which has been in active service for over 40 years, continues to rely on hydrogen peroxide in its gas generator to drive the main turbine pump and in the reaction control system thrusters used for the descent phase. Much of the British work on hydrogen peroxide (Rothmund and Harlow [8]) was concerned with rocket-assisted takeoff engines for rapid ascent and short runways. This led to several production engines including the monopropellant De Havilland Sprite and the Screamer, dating back to 1956.

The most significant technological challenge for the realization of hydrogen peroxide monopropellant thrusters is the development of effective, reliable, long-lived catalytic beds providing fast and

Presented as Paper 5465 at the 43rd AIAA/ASME/SAE/ASEE Joint Propulsion Conference & Exhibit, Cincinnati, OH, 8–11 July 2007; received 28 June 2007; revision received 7 January 2008; accepted for publication 11 January 2008.

*Ph.D. Student, Aerospace Engineering Department, Pisa University; also Project Engineer, Via Gherardesca 5, Ospedaletto; a.pasini@alta-space.com. Member AIAA.

†Project Manager, Via Gherardesca 5, Ospedaletto; l.torre@alta-space.com. Member AIAA.

‡Project Engineer, Via Gherardesca 5, Ospedaletto; l.romeo@alta-space.com. Member AIAA.

§Project Manager, Via Gherardesca 5, Ospedaletto; a.cervone@alta-space.com. Member AIAA.

¶Professor, Aerospace Engineering Department, Pisa University; luca.dagostino@ing.unipi.it. Member AIAA.

repeatable performance, insensitivity to poisoning by the stabilizers and impurities contained in the propellant, capable of sustaining the large number of thermal cycles imposed by typical mission profiles, and not requiring (if possible) preheating for efficient operation. Nowadays, the most-used catalyst materials for H_2O_2 are metallic silver (Runckel et al. [6]; Morlan et al. [9]), permanganates of alkali metals as in Musker [10], and manganese oxides (typically MnO_2 and Mn_2O_3). Some experience is also available with alumina-deposited platinum, ruthenium dioxide, divanadium pentoxide, and lead oxide, as in Rusek [11]. None of these solutions is free from drawbacks, the most important being temperature limitations and poisoning for metallic silver (Wernimont and Mullens [12]; Ventura and Wernimont [13]), powdering and thermomechanical resistance for ceramic-deposed catalysts, excessive flow resistance for pellet beds, and flow stratification for channel matrix support catalysts (Beutien et al. [14]).

Along with the application of hydrogen as a monopropellant, there was also an evolution of the methods used for catalyst decomposition and development. The workhorse catalyst for 90% hydrogen peroxide has long been the silver screen pack [13]. This catalyst proved to be a robust choice, but its relatively low melting temperature limits its use to hydrogen peroxide concentrations lower than about 92%. Earlier 98% HP catalytic beds, realized in the 1950s and 1960s, were based on the use of screens made of different materials, such as high melting point silver alloys (silver palladium), platinum, palladium, iridium, ruthenium, manganese dioxide, and cobalt. However, no one of these candidate materials provided really adequate performance. Alternative techniques for decomposing hydrogen peroxide greater than 90% are necessary to fully exploit the higher performance offered by 98% H_2O_2.

Kappenstein et al. [15] have recently investigated the thermal decomposition and the hydrothermal reduction of different permanganate precursors of manganese oxide-based catalysts, finding that a higher reaction surface area and activity are exhibited when using potassium permanganate rather than sodium permanganate. An extensive experimental study carried out by Rusek [11] indicated that catalysts based on MnO_2 or Mn_2O_3 on different ceramic pellets led to an activity about 1 order of magnitude higher than obtained with silver. Other catalysts, such as ruthenium dioxide, displayed activities about 3 times higher than manganese oxides. Moreover, a series of thermal tests in the same study showed that the activity of platinum on alumina is 1 order of magnitude higher than exhibited by manganese oxides-based catalysts. These findings, however, are not fully consistent with those obtained by Pirault-Roy et al. [16], who investigated the activity of platinum supported on silica, silver, and iridium and platinum-tin or manganese oxides supported on alumina, observing that silver on alumina yielded the highest activity, followed by manganese oxides on alumina and by platinum on silica. Another experimental activity was carried out by Eloirdi et al. [17] using a constant-volume batch reactor. Two catalysts, manganese oxide and silver supported on alumina, were tested. The manganese oxide catalyst showed a better activity with a good repeatability after several firings, whereas the supported silver sample was less active and showed a slight loss of activity after the first firings.

Tian et al. [18] have investigated the performance of the $Ir/\gamma\text{-}Al_2O_3$ catalyst for the decomposition of high-concentration hydrogen peroxide in a monopropellant thruster, finding that catalyst oxidation and surface Sn poisoning are the main reasons for catalyst deactivation. Beutien et al.[14] have illustrated the evaluation of cordierite-based catalytic beds for 98% hydrogen peroxide. The most interesting characteristic of cordierite as a catalyst supporting material, together with its relatively good mechanical strength, is that it does not melt or break when exposed to 98% hydrogen peroxide decomposition. Furthermore, high-channel density catalytic beds tend to result in higher temperatures and a more complete decomposition with respect to low pore density ones (Long and Rusek [19]).

As a direct consequence of the renewed interest in the use of hydrogen peroxide by the rocket propulsion community, the use of advanced catalytic beds for the development of hydrogen peroxide monopropellant rocket thrusters has been investigated by the authors. The objective of the activity presented in this paper was the design and realization of two prototype thrusters (a 5 N one and a 25 N one), for which catalytic beds made of different catalyst materials and substrates could be installed and validated. The present paper illustrates the performance of $Pt/\gamma\text{-}Al_2O_3$ catalysts in the 5 N thruster prototype.

II. Test Apparatus

A. Engine Test Bench and Propellant Feed System

The experimental characterization of the 5 N thruster prototype has been carried out using the Hydrogen Peroxide Thrusters Test Facility. It consists of a custom-made test bench and a propellant feed system, designed for providing hydrogen peroxide to the thruster prototypes.

A three-dimensional view of the test bench is shown in Fig. 1. The mobile part of the 1-degree-of-freedom dynamometric force balance for the measurement of the engine's axial thrust consists of an L-shaped cradle, obtained by bolting together a horizontal and a vertical plate by means of two lateral triangular ribs. The load cell for the measurement of the axial thrust is installed on the vertical plate. The engine prototype is mounted in the cradle, which has suitable provisions for the hydrogen peroxide feed line and for accommodating thrusters of different sizes. The engine cradle is connected to the upper supporting plate of the thrust balance by means of two flexures realized out of 0.05-mm-thick stainless steel sheets. These flexures are designed for transmitting to the supporting structure all of the off-axis engine loads, while being extremely flexible in the axial direction to minimize their interference with the thrust measurement. For bigger thrusters, it is possible to easily reconfigure the balance over a relatively wide range of thrust levels by simply mounting a cell with a suitable load capacity and by changing the thickness of the flexures. The thrust balance is suspended to a stiff cantilever beam supported by a second vertical I beam, which also mounts the stop plate and screw used as mating elements for adjusting the compression preload of the measuring cell. The test bench has been designed with particular attention to the reduction of spurious additional forces interfering with the thrust measurement. The calibration showed that the relative error on the axial thrust introduced by the force balance (i.e., by hydrogen peroxide supply tubes, electrical connections of transducers, flexures, etc.) is lower than 2%.

The propellant feed system has been specifically designed for providing hydrogen peroxide to the prototype thrusters. This system is intended as a multipurpose one, which can easily be adapted and reconfigured for testing thrusters of different operational characteristics (such as bipropellants or hybrids) and target performance. A schematic of the propellant feed system is shown in Fig. 2. High-concentration hydrogen peroxide is stored at up to 40 bar pressure in the main 2.5 liter tank made of stainless steel and internally coated with Teflon. If necessary, its storing capability can be increased by connecting it to a larger tank. To avoid dangerous overpressures in the case of uncontrolled hydrogen peroxide decomposition, the tank is connected to a manually operated safety valve, a burst disk, and a nonreturn valve. The physical conditions of the propellant stored in

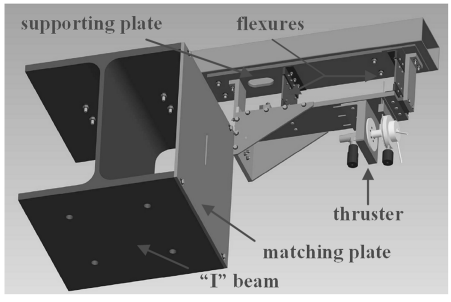

Fig. 1 3-D drawing of the test bench assembly.

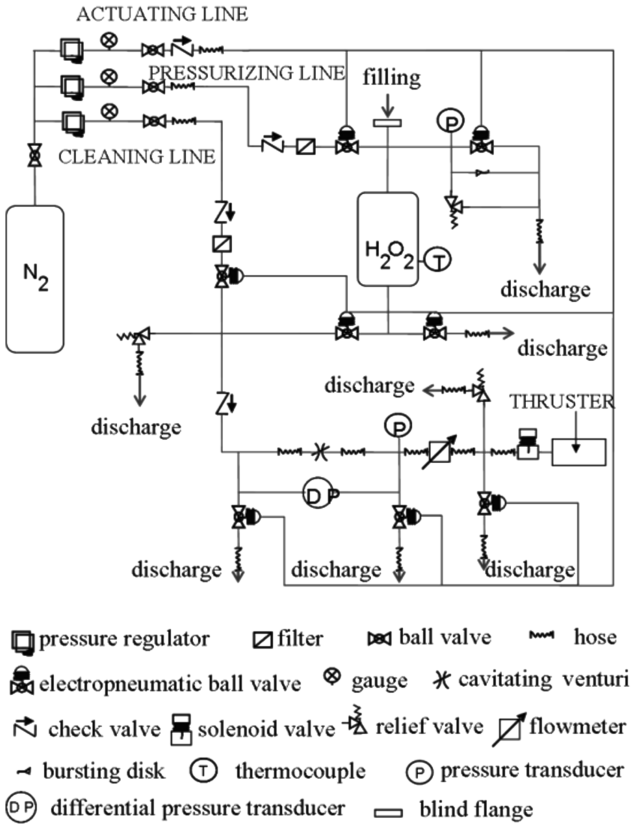

Fig. 2 Schematic of the hydrogen peroxide supply facility.

the tank are monitored by means of a thermocouple [6-mm-diam J-type mineral-insulated thermocouple) and a pressure transducer (0–40 bar pressure range and an accuracy of 0.43% full scale output (FSO)]. A check valve, a cavitating venturi (0.254 mm throat diameter), and a Coriolis flowmeter (with a maximum operating pressure of 150 bar, a maximum flow rate of 100 kg/hr, and an accuracy of 0.1% of the measured flow rate) have been placed along the hydrogen peroxide feeding line to, respectively, prevent flow reversals, regulate the flow by only adjusting the upstream pressure in the tank, and monitor the propellant mass flux with the required accuracy. For ease of reconfiguration, standard (1/4 in.) polytetrafluoroethylene-lined, stainless-steel-braided hoses have been used for interfacing the main components of the feed system. Remotely operated electropneumatic valves have been employed for operating the various fluid lines of the facility. A commercial solenoid valve with a low response time (<20 ms) has been chosen as a firing valve. Gaseous nitrogen from a 200 bar bottle has been fed at different regulated pressures to the three lines used for propellant tank pressurization (40 bar) and pneumatic valve actuation (7–8 bar), and for purging to a discharge tank and venting all of the hydrogen peroxide lines.

To prevent accidents, the detailed test procedure has been specified in written step-by-step instructions and the team has been equipped with the personal protective equipment prescribed when handling high-grade hydrogen peroxide.

B. 5 N Thruster Prototype

The thruster has been designed in a modular manner (Cervone et al. [20]) and consists of five main components in AISI 316L stainless steel (see Fig. 3): the catalytic bed, the nozzle, the connecting flange, the injection plate, and the distribution plate. Sealing is obtained by means of copper-coated Inconel C rings, and two AISI 304 stainless steel screens (37 × 37 mesh size and 0.2 mm wire diameter) are used for retaining the catalyst pellets.

The sizing of the engine prototype and its components has been carried out using the standard simplified isentropic 1-D relations presented in Cervone et al. [20]. The chamber pressure, the residence

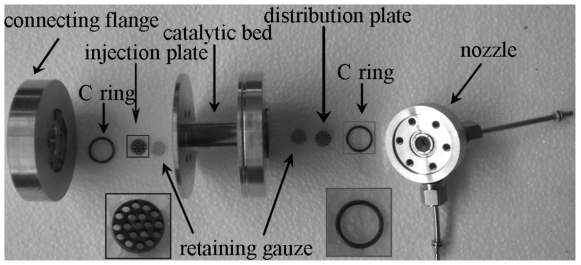

Fig. 3 Main parts of the thruster prototype.

time of the propellant in the catalytic bed, and the catalytic bed loading have been chosen based on the typical values reported in the open literature for similar applications. Originally, the conical nozzle was designed for an exhaust pressure of 13,800 Pa. Because the tests reported in this paper would have been carried out at atmospheric external pressure, the original nozzle has been shortened to avoid flow separation due to excessive overexpansion. Table 1 summarizes the main features of the 5 N test thruster.

C. Measurements and Data Acquisition System

The measurements taken during a typical test can be divided into two different categories: measurements for monitoring the operation of the propellant supply system and measurements for evaluating the performance of the thruster prototype.

With reference to Fig. 2, three pressure transducers, one thermocouple, and one flowmeter have been installed along the hydrogen peroxide line to carry out the following measurements: 1) the tank delivery pressure, which is directly related to the propellant mass flow rate as long as cavitating conditions are established in the venturi; 2) the tank temperature, whose abnormal increase is usually an indication of incipient decomposition of the stored hydrogen peroxide; 3) the venturi differential pressure, whose value is indicative of correct operation under cavitating conditions in which the hydrogen peroxide mass flow rate only depends on the tank delivery pressure; 4) the venturi outlet pressure, which gives information on the state of the fluid entering the flowmeter and indirectly on the venturi inlet pressure; and 5) the propellant flow rate.

Figure 4 shows a schematic of the 5 N thruster prototype and the transducers' arrangement as described in the Sec. II.B. To monitor the performance of the thruster prototype the following measurements are taken: 1) the thruster inlet pressure, by means of a pressure transducer with a maximum combined error (nonlinearity, hysteresis, and repeatability) of 1% FSO, mounted using an adapter on the "T" junction placed just in front of the injection plate; 2) the chamber pressure, by means of a second pressure transducer mounted by means of a suitable connector to the tube brazed on the converging portion of the nozzle; 3) the chamber temperature, by means of a 0.5-mm-diam K-type mineral-insulated thermocouple

Table 1 Main characteristics of the test thruster

		Units	Values
Propellant	H_2O_2 content	g/100 g	87.5
	Tin content	ppm	5–9
	Phosphate content (as PO_4)	ppm	≤ 0.5
Catalytic bed	Inner diameter	mm	8
	Length/diameter ratio	——	4
Nozzle	Throat diameter	mm	2
	Exhaust diameter	mm	3.73
	Exhaust area ratio	——	3.48
	Conical nozzle half-angle	deg	15
	Nozzle length	mm	3.23
Inj./dist. plates	Diameter	mm	8
	Diameter of holes	mm	1.5
	Open area/total area ratio	——	0.5

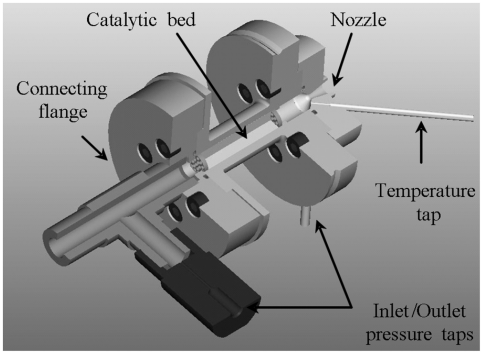

Fig. 4 Cutoff assembly drawing of the thruster prototype.

inserted in the dedicated temperature tap; and 4) the thrust, by means of a subminiature compression load cell with 1 kgf full scale output (1 kgf = 9.807 N) and a maximum combined error (nonlinearity, hysteresis, and repeatability) of 0.9% FSO.

A dc source, capable of supplying different output voltages, provides the transducers with the required excitations. The data coming from the sensors and transducers installed in the facility are acquired and transferred to a personal computer by means of an acquisition board capable of acquiring 32 analogical and 48 digital channels at a maximum sample rate of 1.25 MSamples/s. The acquisition board is connected to 1) a module for conditioning and filtering the signals coming from the pressure transducers, the load cell, and the flowmeter; 2) a module for conditioning and filtering the thermocouple signals; and 3) a module for providing the digital outputs for the remote control of the electropneumatic valves.

In particular, the flowmeter current output (4–20 mA) has been changed into a voltage output by means of a calibrated 200 Ω resistance (0.8–4 V) to acquire the signal using the same module.

A data acquisition and control program has been implemented. The operator can actuate the valves both manually (by clicking on the corresponding display switch) and automatically (by starting the predefined automatic procedures), having direct knowledge of the state of the valves. The acquired data are recorded and real-time displayed on the front panel. Separate windows also allow for an in-line display of the time histories of all of the main measurements acquired during the test. This allows the operator to fully monitor the entire system and make the proper decisions. Before the program is run, it is also necessary to choose the sample acquisition rate compatible with the maximum sampling rate of the acquisition board and the CPU performance. A value of 10 Samples/s has been selected for the tests reported in this paper.

III. Catalysts

The core of the hydrogen peroxide monopropellant thruster is represented by the catalyst. A series of advanced catalysts on ceramic supporting spheres based on novel implantation techniques have been developed. The chemical activity of these catalysts has been preliminarily assessed using a 30% hydrogen peroxide solution by weight in a dedicated test bench [21,22] to select the most promising catalysts to be integrated in the thruster prototype. Two platinum-based catalysts, obtained from two different precursors (marked as the first and second type in Table 2) using the same γ-alumina carrier and deposition procedure, have been selected, as they proved to be very active and relatively insensitive to poisoning problems.

The preparation technique for the catalysts was based on the following steps: impregnation at 20°C, washing with pure solvent, filtration, drying in vacuo (10^{-4} atm) at room temperature, and reduction under hydrogen at 130°C for 2 h. The catalysts were obtained from the same carrier, but using different precursors. Before impregnation, the ceramic support was dried in vacuo (10^{-4} atm) at 140°C. The nominal metal loading on the catalyst was 3.99 (mol $\times$ 10^3) for the LR-57 catalyst and 3.82 (mol $\times$ 10^3) for the LR-59 catalyst.

The last column in Table 2 reports the catalyst load expressed in percent atomic content (at. %), which refers to the average scanning electron microscopy (SEM) reading over the optical framing window (200×180 μm) down to the typical penetration depth of the electron beam below the catalyst surface (about 200 atomic layers). The lighter external layer in the sphere cross section of the LR-59 catalyst shown in Fig. 5 (bottom) indicates the depth of the platinum deposition, which extends down to 180 μm below the surface, about half of the pellet radius. The color of the external surface does not show important solution of continuity, thus suggesting that the platinum distribution is uniform.

IV. Experimental Results and Discussion

Two catalytic beds made with the LR-57 and LR-59 platinum-deposed ceramic spheres of Table 2 have been tested in the monopropellant thruster prototype. Both catalysts have decomposed hydrogen peroxide at concentration of 87.5%. For one of them, experimental data on the operation with 70% hydrogen peroxide are also available. For ease of assessment, the performance of these catalytic beds has been compared with that of a conventional silver screen catalytic bed of equal geometric envelope (diameter and length).

A. Performance Definition and Theoretical Evaluation

These tests have been mainly used to evaluate the behavior of the catalytic beds. In propulsive applications, the characteristic velocity efficiency ("C-Star efficiency") represents a significant parameter closely related to the capability of the catalytic bed of effectively decomposing the propellant for generating thrust. This parameter is based on the quasi-1-D theory of ideal rocket performance (perfect gas with constant composition, quasi-1-D steady isentropic frictionless flow, critical throat, and negligible velocity in the combustion chamber) and compares the characteristic velocity obtained from the measurements of the propellant mass flow rate and chamber pressure with the theoretical value computed for a chamber temperature and composition corresponding to complete adiabatic decomposition of the propellant:

Table 2 Main characteristics of the catalytic systems used in the thruster experiments

ALTA's code	LR-57	LR-59
Catalyst	Platinum first type	Platinum second type
Carrier	*SASOL 06/170 γ-alumina spheres* Diameter: 0.6 mm Surface area: 170 m^2/g Pore volume: 0.53 ml/g Al_2O_3: 96.1%	
Deposition procedure	1) Impregnation phase (Pt precursor and solvent) 2) Drying phase (mechanical depressurization at 10^{-4} atm and room temperature) 3) Reduction phase (under hydrogen atmosphere at room temperature)	
SEM at. %	0.39	0.47

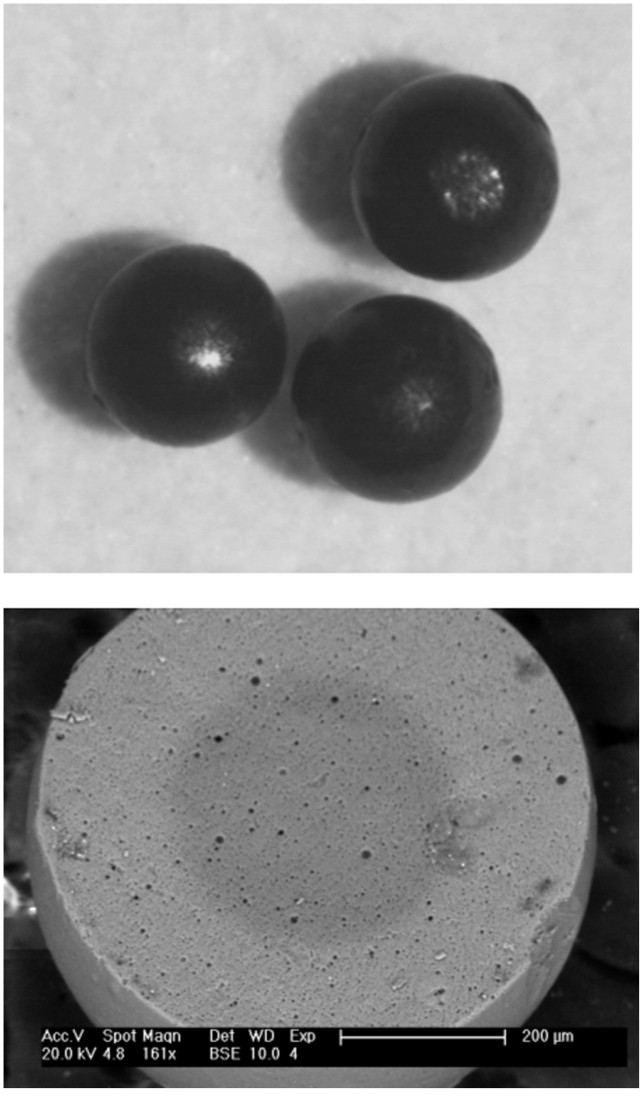

Fig. 5 LR-59 catalytic spheres (top) and SEM picture at 161x magnification (bottom).

$$\eta_{c^*_{T_{\text{ad}}}} = \frac{c^*_{\text{exp}}}{c^*_{T_{\text{ad}}}} = \frac{\frac{p_{c_{\text{exp}}} A_t}{\dot{m}_{\text{exp}}}}{\sqrt{\frac{R_{T_{\text{ad}}} T_{\text{ad}}}{\gamma_{T_{\text{ad}}}}} \left(\frac{\gamma_{T_{\text{ad}}}+1}{2}\right)^{\frac{\gamma_{T_{\text{ad}}}+1}{2(\gamma_{T_{\text{ad}}}-1)}}} \tag{1}$$

A second significant parameter is the "temperature efficiency," which expresses how close the measured chamber temperature is to the adiabatic temperature corresponding to complete decomposition of the propellant:

$$\eta_{\Delta T} = \frac{T_{\text{exp}} - T_{\text{amb}}}{T_{\text{ad}} - T_{\text{amb}}} \tag{2}$$

To evaluate the deviation of the real behavior of the propellant gas in the thrust chamber from the theoretical one, it has been decided to employ the aforementioned definition of the C-Star efficiency, in which the reference characteristic velocity is computed from the experimental values of the chamber temperature and composition:

$$\eta_{c^*_{T_{\text{exp}}}} = \frac{c^*_{\text{exp}}}{c^*_{T_{\text{exp}}}} = \frac{\frac{p_{c_{\text{exp}}} A_t}{\dot{m}_{\text{exp}}}}{\sqrt{\frac{R_{T_{\text{exp}}} T_{\text{exp}}}{\gamma_{T_{\text{exp}}}}} \left(\frac{\gamma_{T_{\text{exp}}}+1}{2}\right)^{\frac{\gamma_{T_{\text{exp}}}+1}{2(\gamma_{T_{\text{exp}}}-1)}}} \tag{3}$$

This efficiency takes into account viscous effects and the other sources of losses and inefficiencies that are not considered in the quasi-1-D model of ideal rocket performance.

Finally, in space propulsion applications the pressure drop across the catalytic bed is another important operational parameter because of its obvious repercussions on the propellant pressurization and indirectly on the design of the entire feed system. Bed pressure losses depend on the flow configuration and operating conditions (bed porosity, length, loading, flow pressure, and temperature) and, in general, must be reduced to minimize the mass of the propellant feed system. Later results compare the pressure drop measured at the same operational conditions in catalytic beds realized by means of spherical pellets with those obtained in silver screen reactors of equal geometric envelope (diameter and length).

In the following sections, to characterize the propulsive performance of the engine prototype, the measured time evolution of the thrust and the chamber pressure have been compared with the theoretical values obtained from the quasi-1-D model of ideal rockets. Based on the experimental results, it has also been possible to evaluate the thrust coefficient and the specific impulse using the well-known expressions:

$$C_{F_{\text{exp}}} = \frac{F_{\text{exp}}}{p_{c_{\text{exp}}} A_t} \qquad I_{\text{sp}_{\text{exp}}} = \frac{c^*_{\text{exp}} C_{F_{\text{exp}}}}{g_o} \tag{4}$$

B. 70% H_2O_2 Firing

In the first test, the tank has been filled with 450 ml of 70% hydrogen peroxide and a single, relatively long firing has been carried out up to complete depletion of the tank. The mass flow rate of hydrogen peroxide has been controlled using the cavitating venturi, previously calibrated with bidistilled water to identify its effective throat area. The use of the cavitating venturi also allowed for the reliable measurement of the mass flow rate, in spite of a temporary malfunction of the Coriolis flowmeter.

The firing comprised an initial transient phase (lasting about 12 s), a longer steady-state operation (lasting about 75 s), followed by the progressive occlusion of the catalytic bed due to the thermal rupture of the ceramic pellets. Measurements of the thrust chamber parameters indicated the occurrence of large-amplitude oscillations about their mean values due to the onset of a flow instability. Because the data have been acquired at 10 Samples/s without analog filtering, the unstable frequency, which was higher than the Nyquist frequency corresponding to the acquisition rate [23], could not be resolved by Fourier analysis of the acquired signals. A moving average has therefore been used to smooth out short-term fluctuations, to digitally simulate low-pass filtering of the acquired data. The theoretical and the experimental values of the thrust are shown in Fig. 6, whereas their steady-state values are summarized in Table 3 together with the other main operational parameters of the catalytic bed. Two theoretical values of the thrust are presented: the first one is evaluated using the expected adiabatic chamber temperature, whereas for the second one the actual temperature measured during the experiment is used. The bed loading and chamber pressure were 76.6 kg/s/m^2 and 6 bar, respectively. Figure 7 shows the C-Star efficiency. The low values of the decomposition temperature and, consequently, of the C-Star and temperature efficiencies that characterize the catalyst behavior clearly indicate the incomplete decomposition of hydrogen peroxide as the main reason for the attainment of relatively poor propulsive performance. On the other hand, during the steady-state phase the pressure drop across the catalytic bed reached 4 bar, a relatively high value. Later in the run (at the relative time 5980 s), the pressure losses started to increase even further, due to the progressive occlusion of the catalytic bed (see Fig. 8). The step line in Figs. 6–8 indicates the opening time of the thruster valve; a higher value means "open" and a lower value means "closed."

C. 87.5% H_2O_2 Firings

The Pt/ Al_2O_3 second type (LR-59) catalyst has also been tested in the engine prototype with the same procedure using higher grade 87.5% hydrogen peroxide. During the first firing, the catalytic bed started to occlude just a few seconds after the reaching steady-state

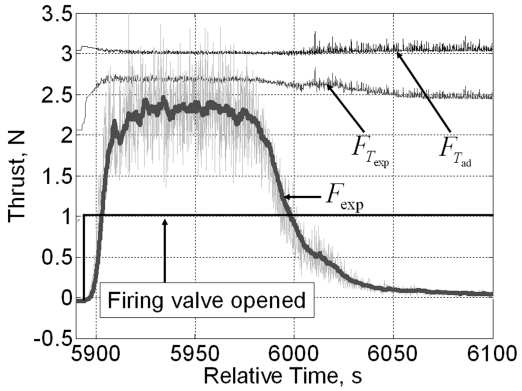

Fig. 6 Thrust: theoretical values (evaluated using both the expected adiabatic temperature and the actually measured chamber temperature) and the experimental measurement (LR-59, 70% H_2O_2).

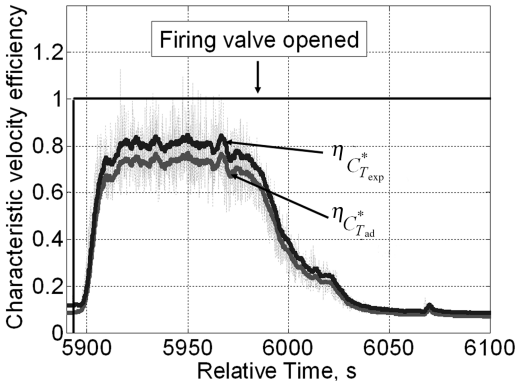

Fig. 7 C-Star efficiency, evaluated using both the expected adiabatic temperature and the actually measured chamber temperature (LR-59, 70% H_2O_2).

operation, and the firing had to be terminated. Later attempts to restart the thruster have been unsuccessful.

All experimental data have been low-pass filtered by means of a 10 Hz cutoff frequency analog Butterworth filter and acquired at 10 Samples/s, thereby eliminating the need to use the moving average in the reduction of the data. Figure 9 shows the theoretical and experimental values of the thrust, Fig. 10 shows the characteristic velocity efficiency, and Fig. 11 shows the bed pressure drop. Figure 9, in particular, indicates that the initial transient phase of the test run lasted for about 10 s, while steady-state operation has only been attained for a few seconds. However, even this short period of time has been sufficient for the evaluation of the steady-state conditions, summarized in Table 4.

The operating parameters of the catalytic bed were very similar to the previous firing using 70% hydrogen peroxide. In particular, the chamber pressure was 5.5 bar and the bed loading 73.2 kg/s/m^2. Not surprisingly, the chamber pressure and thrust display quite similar trends. Also in this case, their relatively low values are due to the incomplete decomposition of hydrogen peroxide, as indicated by the temperature efficiency, 62%, and the characteristic velocity efficiency, 52%.

The starting time of the occlusion of the catalytic bed can be easily identified from the diagram in Fig. 11 as the inflection point at which the pressure drop starts to increase suddenly. As a consequence of bed occlusion when using the Pt/ Al_2O_3 second type catalyst (LR-59), several tests with high-grade hydrogen peroxide have been carried out in a dedicated catalytic activity facility [21,22] to identify the most promising substitute. ThePt/ Al_2O_3 first type catalyst (LR-57) proved to be the least sensitive to pellet rupture and, therefore, has been tested in the engine prototype under the same operating conditions as the LR-59 bed reactor.

A total of 275 ml of 87.5% H_2O_2 have been used, acquiring the experimental data at 10 Samples/s without filtering. Also in this case, a moving average has been employed to smooth out short-term fluctuations. Figures 12–14, together with Table 5, show the results of this test. The data of Table 5 indicate that the performance of the

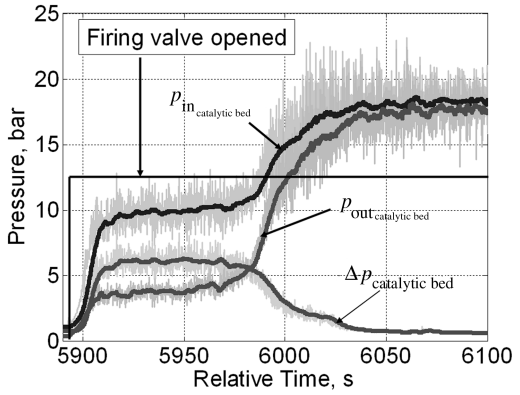

Fig. 8 Catalytic bed pressure drop (LR-59, 70% H_2O_2).

LR-57 catalyst bed turned out to be slightly better than that of the LR-59 catalyst. In particular, the characteristic velocity efficiency (Fig. 13) improved because the chamber pressure had increased (see Table 5). Unfortunately, the occlusion of the catalytic bed still occurred. The steady-state operation lasted almost twice as long as in the previous case (10 s), but the pressure drop across the bed also dramatically increased (see Fig. 14).

Finally, Table 6 summarizes the steady-state performance of a silver screen catalytic bed with the same envelope dimensions (diameter and length) and tested at equal operating conditions as the previous pellet reactors. A total of 140 silver screens (99.9% purity) with a 80 × 80 in.$^{-2}$ mesh size and a wire diameter of 0.115 mm have been used as catalyst.

The decomposition efficiency, the characteristic velocity efficiency, and the temperature efficiency were significantly higher than for the previous pellet reactors, but still far from their theoretical limits, most likely as a consequence of insufficient bed length and possibly because of the occurrence of flow channeling phenomena. The increase in the decomposition temperature allowed for a higher

Table 3 Steady-state performance with the LR-59 catalyst and 70% H_2O_2

Performance	5 N thruster (LR-59)	Ideal adiabatic decomposition
Thrust	2.3 N	3.0 N
Chamber pressure	6 bar	8.5 bar
Chamber temperature	433 K	514 K
Mass flow rate	3.85 g/s	3.85 g/s
Characteristic velocity	500 m/s	680 m/s
Thrust coefficient	1.16	1.16
Specific impulse	60 s	80 s
Bed loading	76.6 kg/s/m^2	76.59 kg/s/m^2
c^* efficiency	0.73	——
ΔT efficiency	0.60	——
Catalytic bed pressure drop	4 bar	——

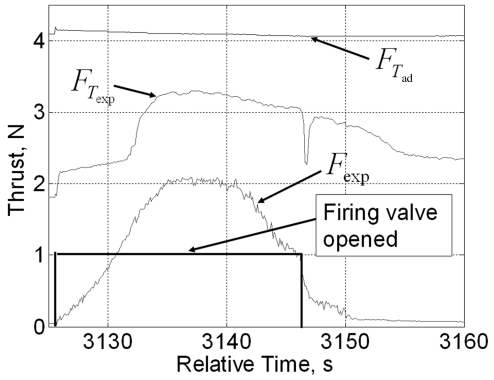

Fig. 9 Thrust: theoretical values (evaluated using both the expected adiabatic temperature and the actually measured chamber temperature) and the experimental measurement (LR-59, 87.5% H_2O_2).

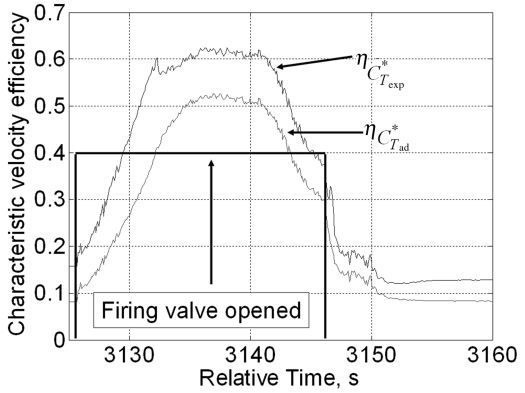

Fig. 10 C-Star efficiency, evaluated using both the expected adiabatic temperature and the actually measured chamber temperature (LR-59, 87.5% H_2O_2).

value of the chamber pressure and, consequently, a higher thrust. Furthermore, the pressure drop through the bed turned out to be lower than for the previous ceramic pellet reactors.

V. Conclusions

The current design of HP catalytic reactors based on novel catalyst implantation techniques on γ-alumina ceramic supports has led to unsatisfactory levels of performance. The main problems encountered can be summarized as follows: 1) rupture of the pellets and consequent occlusion of the catalytic bed; 2) low c^* and temperature efficiencies; 3) onset of catalyst bed flow instabilities; and 4) high pressure drop across the catalytic bed.

Preliminary analyses of the relevant physical phenomena by means of reduced order models suggested that the main causes of these problems can be tentatively identified as follows:

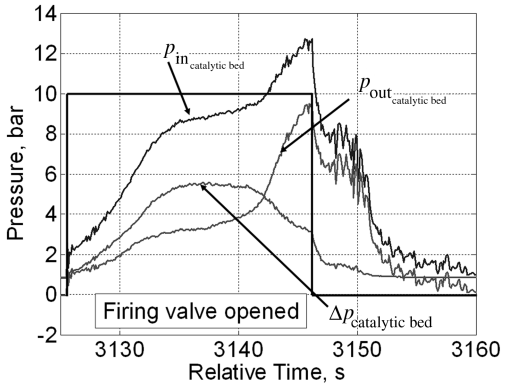

Fig. 11 Catalytic bed pressure drop (LR-59, 87.5% H_2O_2).

1) The rupture and powdering of the catalyst pellets was due to excessive thermal stresses induced by the rapid and large change of their surface temperature during the initial phase of hydrogen peroxide decomposition. The occurrence of either one of these cracking modes seems to depend on the intensity of the superficial heat release and the ensuing different evolution of the radial temperature profile in the catalyst pellets.

2) The progressive occlusion of the bed by the debris was generated by the thermal cracking of the catalyst pellets.

3) The mass diffusion limitations of the decomposition rate was due to the large velocity difference between the incoming liquid reactant and the outgoing gaseous products, which effectively reduce the c^* and temperature efficiencies below the theoretical values.

4) The flow channeling, whose occurrence is suggested by the observed occurrence of fluid dynamic instabilities in the reactor, is known to interfere with the spatial distribution and intensity of hydrogen peroxide decomposition, with the consequence that the pressure drop in the reactor becomes very sensitive to changes of the H_2O_2 flow rate. Any accidental decrease of the decomposition rate results in a temporary increase of the liquid hydrogen peroxide concentration and flow velocity, due to the parallel decrease of the pressure losses. As soon as the local accumulation of hydrogen peroxide eventually succeeds in increasing the decomposition rate, the liquid is replaced by faster gaseous products and the flow velocity increases, preparing the conditions for the next oscillation cycle.

The identification of the physical causes of the problems affecting the catalytic reactor provides some guidelines in finding possible solutions. Stratified or multiple beds with increasing decomposition activity in the flow direction can conceivably reduce thermal stresses down to sustainable levels, at the expense, however, of larger bed volumes and higher pressure losses. Mechanical analyses of thermal loads in the catalyst pellets suggests that the cracking of the catalyst support, and the consequent occlusion of the reactor, might be avoided by using ceramic materials with higher thermal shock resistance. Four ways of pursuing this objective have been identified: 1) reducing the product of the thermal expansion coefficient times the Young's modulus of the supporting material; 2) increasing the ultimate stress of the supporting material; 3) increasing the thermal

Table 4 Steady-state performance with the LR-59 catalyst and 87.5% H_2O_2

Performance	5 N thruster (LR-59)	Ideal adiabatic decomposition
Thrust	2.05 N	4.1 N
Chamber pressure	5.5 bar	10.5 bar
Chamber temperature	703.15 K	952.85 K
Mass flow rate	3.68 g/s	3.68 g/s
Characteristic velocity	470 m/s	904 m/s
Thrust coefficient	1.20	1.23
Specific impulse	57 s	113 s
Bed loading	73.21 kg/s/m^2	73.21 kg/s/m^2
c^* efficiency	0.52	——
ΔT efficiency	0.62	——
Catalytic bed pressure drop	3.2 bar	——

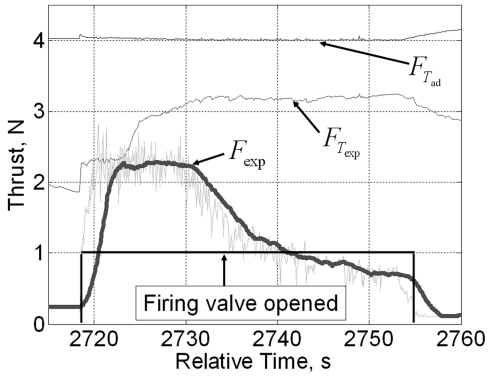

Fig. 12 Thrust: theoretical values (evaluated using both the expected adiabatic temperature and the actually measured chamber temperature) and the experimental measurement (LR-57, 87.5% H_2O_2).

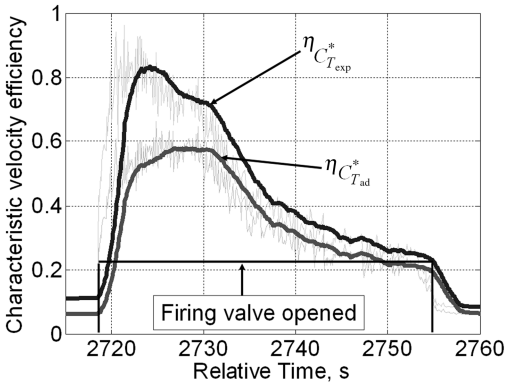

Fig. 13 C-Star efficiency, evaluated using both the expected adiabatic temperature and the actually measured chamber temperature (LR-57, 87.5% H_2O_2).

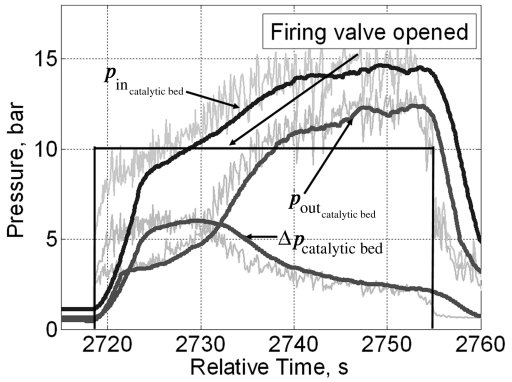

Fig. 14 Catalytic bed pressure drop (LR-57, 87.5% H_2O_2).

conductivity of the supporting material; and 4) decreasing the typical thickness of the supporting material.

If susceptible to effective catalyst deposition, cordierite, titania, zirconia, silicon nitride, and silicon carbide are some potentially interesting ceramic materials for catalyst support. As an example, monolithic ceramic catalysts have been effectively tested by Scharlemann et al. [24]. The catalysts presented in their work were manufactured with a wash coating procedure and following impregnation, using mullite and mullite-zirconia monolithic cellular ceramics as substrates and an aqueous solution of sodium permanganate (NaMnO4) as a precursor. Up to 1.2 kg of hydrogen peroxide could be decomposed by the most promising catalyst reported in this work.

Two other important parameters are the intensity and distribution of thermal stresses, which are a strong function of the pellet Biot number hD/k when its value is of order unity. Because the superficial heat release due to hydrogen peroxide decomposition can be expressed in terms of an effective heat transfer coefficient, the reduction of the pellet size can also effectively contribute to mitigate the thermal stress problem of the catalyst support.

Several actions can be undertaken to improve the decomposition activity of the catalytic bed: 1) increasing the active area of the

Table 5 Steady-state performance with the LR-57 catalyst and 87.5% H_2O_2

Performance	5 N thruster (LR-57)	Ideal adiabatic decomposition
Thrust	2.3 N	4.1 N
Chamber pressure	6 bar	10.5 bar
Chamber temperature	703.15 K	952.85 K
Mass flow rate	3.68 g/s	3.68 g/s
Characteristic velocity	520 m/s	904 m/s
Thrust coefficient	1.20	1.23
Specific impulse	65 s	113 s
Bed loading	73.2 kg/s/m^2	73.2 kg/s/m^2
c^* efficiency	0.58	——
ΔT efficiency	0.62	——
Catalytic bed pressure drop	6 bar	——

Table 6 Steady-state performance with the silver screen catalyst and 87.5 % H_2O_2

Performance	5 N thruster (silver grids)	Ideal adiabatic decomposition
Thrust	3 N	4.0 N
Chamber pressure	7 bar	10.5 bar
Chamber temperature	773.15 K	952.85 K
Mass flow rate	3.62 g/s	3.62 g/s
Characteristic velocity	724 m/s	904 m/s
Thrust coefficient	1.22	1.23
Specific impulse	80 s	113 s
Bed loading	72.00 kg/s/m^2	72.00 kg/s/m^2
c^* efficiency	0.80	——
ΔT efficiency	0.72	——
Catalytic bed pressure drop	2 bar	——

catalyst by means of longer beds or a smaller pellet size, accepting the associated pressure loss penalty; 2) increasing the catalyst deposition on the support; and 3) increasing the reactant concentration by raising the flow pressure.

The results of 1-D steady analyses of the two-phase homogeneous reacting flow through the catalytic bed indicate that the last alternative might be particularly attractive because of its positive combined influence on the decomposition rate of hydrogen peroxide in the gaseous phase, on the propulsive efficiency of the engine, and on the pressure losses through the reactor. Flow instabilities can probably be suppressed by the introduction in the catalytic bed of flow redistribution elements capable of negatively interfering with channeling phenomena, even though it's at the expense of increased pressure losses.

Acknowledgments

The present work has been funded under contract no. 18903/05/NL/DC by ESA–European Space Research and Technology Centre in the framework of the Leading Edge Technologies for Small and Medium Sized Enterprises (LET–SME) program, whose support is gratefully acknowledged. The authors would like to express their gratitude to Mariano Andrenucci, Fabrizio Paganucci, and Renzo Lazzeretti of the Dipartimento di Ingegneria Aerospaziale, Università di Pisa, for their constant and friendly encouragement, and to Antonio D'Elia, Lucio Bruschi, and the other students who contributed to the project.

References

[1] Wernimont, E., and Mullens, P., "Recent Developments in Hydrogen Peroxide Monopropellant Devices," AIAA Paper 99-2741, June 1999.

[2] Wernimont, E., and Garboden, G., "Experimentation with Hydrogen Peroxide Oxidized Rockets," AIAA Paper 99-2743, June 1999.

[3] Wucherer, E. J., Christofferson, S., and Reed, B., "Assessment of High Performance HAN Monopropellants," AIAA Paper 2000-3872, July 2000.

[4] Schoyer, H. F. R., Korting, P. A. O. G., Veltmans, W. H. M., Louwers, J., van der Heijden, A. E. D. M., Keizers, H. L. J., and van den Berg, R. P., "An Overview of the Development of HNF and HNF-Based Propellants," AIAA Paper 2000-3184, July 2000.

[5] Walter, H., "Hydrogen Peroxide Rockets," *History of German Guided Missile Developments*," AGARDograph, edited by T. Benecke, and A. W. Quick, Vol. 20, Butterworths, London, 1956.

[6] Runckel, J. F., Willis, C. M., and Salters, L. B., Jr., "Investigation of Catalyst Beds for 98-Percent-Concentration Hydrogen Peroxide," NASA TN D-1808, 1963.

[7] Willis, C. M., "The Effect of Catalyst-Bed Arrangement on Thrust Buildup and Decay Time for a 90 Percent Hydrogen Peroxide Control Rocket," NASA TN D-516, 1960.

[8] Rothmund, C., and Harlow, J., "A History of European Liquid-Propellant Rocket Engines for Aircraft," AIAA Paper 1999-2901, June 1999.

[9] Morlan, P., Wu, P., Nejad, A., Ruttle, D., and Fuller, F., "Catalyst Development for Hydrogen Peroxide Rocket Engines," AIAA Paper 1999-2740, June 1999.

[10] Musker, A. J., "Highly Stabilised Hydrogen Peroxide as a Rocket Propellant," AIAA Paper 03-4619, July 2003.

[11] Rusek, J. J., "New Decomposition Catalysts and Characterization Techniques for Rocket-Grade Hydrogen Peroxide," *Journal of Propulsion and Power*, Vol. 12, No. 3, 1996, pp. 574–580.

[12] Wernimont, E., and Mullens, P., "Capabilities of Hydrogen Peroxide Catalyst Beds," AIAA Paper 2000-3555, July 2000.

[13] Ventura, M., and Wernimont, E., "Advancements in High Concentration Hydrogen Peroxide Catalytic Beds," AIAA Paper 01-3250, July 2001.

[14] Beutien, T. R., Heister, S. D., Rusek, J. J., and Meyer, S., "Cordierite-Based Catalytic Beds for Hydrogen Peroxide," AIAA Paper 2002-3853, July 2002.

[15] Kappenstein, C., Pirault-Roy, L., Guèrin, M., Wahdan, T., Ali, A., Al-Sagheer, F., and Zaki, M., "Monopropellant Decomposition Catalysts V. Thermal Decomposition and Reduction of Permanganates as Models for the Preparation of Supported MnO_x Catalysts," *Applied Catalysis A*, Vol. 234, Nos. 1–2, Aug. 2002, pp. 145–153. doi:10.1016/S0926-860X(02)00220-X

[16] Pirault-Roy, L., Kappenstein, C., Guèrin, M., Eloirdi, R., and Pillet, N., "Hydrogen Peroxide Decomposition on Various Supported Catalysts Effect of Stabilizers," *Journal of Propulsion and Power*, Vol. 18, No. 6, 2002, pp. 1235–1241.

[17] Eloirdi, R., Rossignol, S., Chauveau, M., Kappenstein, C., Duprez, D., and Pillet, N., "Design and Use of a Batch Reactor for Catalytic Decomposition of Different Monopropellants," AIAA Paper 00-3553, July 2000.

[18] Tian, H., Zhang, T., Sun, X., Liang, D., and Lin, L., "Performance and Deactivation of Ir/γ-Al_2O_3 Catalyst in the Hydrogen Peroxide Monopropellant Thruster," *Applied Catalysis A*, Vol. 210, Nos. 1–2, March 2001, pp. 55–62. doi:10.1016/S0926-860X(00)00829-2

[19] Long, M. R., and Rusek, J. J., "The Characterization of the Propulsive Decomposition of Hydrogen Peroxide," AIAA Paper 00-3683, July 2000.

[20] Cervone, A., Bramanti, C., d'Agostino, L., Musker, A. J., Roberts, G. T., and Saccoccia, G., "Development of Hydrogen Peroxide Monopropellant Rockets," AIAA Paper 06-5239, July 2006.

[21] Bramanti, C., Cervone, A., Romeo, L., Torre, L., d'Agostino, L., Musker, A, and Saccoccia, G., "Experimental Characterization of Advanced Materials for the Catalytic Decomposition of Hydrogen Peroxide," AIAA Paper 2006-5238, July 2006.

[22] Cervone, A., Romeo, L., Torre, L., d'Agostino, L., Calderazzo, F., Musker, A. J., Roberts, G. T., and Saccoccia, G., "Development of Green Hydrogen Peroxide Monopropellant Rocket Engines and Testing of Advanced Catalytic Beds," *Proceedings of the 3rd International Conference on Green Propellants for Space Propulsion*, SP-635, ESA, Paris, Sept. 2006.

[23] Johnson, C., Anderson, W., and Ross, R., "Catalyst Bed Instability within the USFE H_2O_2/JP-8 Rocket Engine," AIAA Paper 00-3301, July 2000.

[24] Scharlemann, C., Schiebl, M., Marhold, K., Tajmar, M., Miotti, P., Kappenstein, C., Batonneau, Y., Brahmi, R, and Hunter, C., "Development and Test of a Miniature Hydrogen Peroxide Monopropellant Thruster," AIAA Paper 2006-4550, July 2006.

D. Talley
Associate Editor